Measurement of the hydrodynamic corrections to the Brownian motion of two colloidal spheres

John C. Crocker
James Franck Institute and Department of Physics, University of Chicago, Chicago, Illinois 60637

(Received 25 July 1996; accepted 14 November 1996)

The hydrodynamic coupling between two isolated 0.97 μm diameter polystyrene spheres is measured by reconstructing their Brownian motion using digital video microscopy. Blinking optical tweezers are used to facilitate data collection by positioning the spheres in the microscope's focal plane and in close proximity to one another. The observed separation dependence of the spheres' relative and center of mass diffusion coefficients agree with that predicted by low Reynolds number hydrodynamics and the Stokes-Einstein relation. © *1997 American Institute of Physics.* [S0021-9606(97)51307-9]

I. INTRODUCTION

The hydrodynamic interactions between colloidal particles are of tremendous importance to understanding such common colloid phenomena as sedimentation and aggregation. This makes colloidal hydrodynamics relevant to diverse industrial processes, from fluidized beds to blast furnaces, to paper making. Most of the previous experimental work consists of either measurements of the resistance coefficients of macroscopic objects at low Reynolds number,[1–3] the motion of a single microscopic particle near a planar wall,[4–6] or the non-Brownian dynamics of two microscopic spheres colliding in a shear flow.[7] The work presented here concerns the hydrodynamic coupling between two 0.97 μm polystyrene spheres suspended in water, as measured with digital video microscopy. Optical tweezers[8,9] were used to hold the two spheres near each other and in the same focal plane far from the walls of the sample container. The hydrodynamic coupling was measured by its effect, via the Stokes-Einstein relation, on the Brownian diffusivity of the pair of spheres. While the Stokes-Einstein relation has been well established to describe the diffusion of individual particles, there is some theoretical uncertainty regarding its validity in multi-particle systems.[10] This work is uniquely suited to verify the validity of the Stokes-Einstein relation for the two sphere system.

The hydrodynamic forces acting between two spheres at low Reynolds number have been calculated by a number of authors.[11–14] The goal of these calculations is to estimate the resistance to motion felt by a sphere of radius a in a fluid of viscosity η in the presence of a second sphere at a distance r. For a single isolated sphere, motion at a velocity v produces a drag force given by the familiar Stokes formula: $\vec{F}=-(6\pi\eta a)\vec{v}$. The ratio of the velocity to the drag force is termed, in general, the mobility coefficient. When a second sphere is added, the spherical symmetry of the Stokes case is reduced to axial symmetry and four mobility coefficients are needed to quantify the hydrodynamic drag forces. The spheres' motion can be decomposed into two parts: the relative motion of the two spheres with respect to each other and the common motion of the two spheres' center of mass. Each of these two motions are in turn described by a pair of mobility coefficients: one for motion along the line of centers and one for motion perpendicular to it.

These four mobilities can be related to four corresponding diffusion coefficients by a generalized Stokes-Einstein relation. For a single sphere, the Stokes-Einstein relation predicts that the Brownian diffusivity is simply k_BT multiplied by the mobility

$$D_0=\frac{k_BT}{6\pi\eta a}. \tag{1}$$

For two spheres, Batchelor[11] gives asymptotic expressions for the four diffusivities as functions of the dimensionless center-center separation, $\rho=r/a$. If the two spheres have the same radius, no external applied torques, and are free to rotate in response to each other's flow field, the expressions for the diffusion relative to the center of mass are

$$D_{\mathrm{RM}}^{\parallel}=\frac{D_0}{2}\left[1-\frac{3}{2\rho}+\frac{1}{\rho^3}-\frac{15}{4\rho^4}+O(\rho^{-6})\right], \tag{2}$$

$$D_{\mathrm{RM}}^{\perp}=\frac{D_0}{2}\left[1-\frac{3}{4\rho}-\frac{1}{2\rho^3}+O(\rho^{-6})\right], \tag{3}$$

where $D_{\mathrm{RM}}^{\parallel}$ is the diffusivity along the center-center line, and $D_{\mathrm{RM}}^{\perp}$ is perpendicular to it.

The corresponding expressions for the diffusion of the center of mass itself are:

$$D_{\mathrm{CM}}^{\parallel}=\frac{D_0}{2}\left[1+\frac{3}{2\rho}-\frac{1}{\rho^3}-\frac{15}{4\rho^4}+O(\rho^{-6})\right], \tag{4}$$

$$D_{\mathrm{CM}}^{\perp}=\frac{D_0}{2}\left[1+\frac{3}{4\rho}+\frac{1}{2\rho^3}+O(\rho^{-6})\right], \tag{5}$$

where $D_{\mathrm{CM}}^{\parallel}$ is the diffusivity along the center-center line and $D_{\mathrm{CM}}^{\perp}$ is perpendicular to it.

Examination of the lowest order terms indicates that the relative diffusivities are suppressed while the center of mass diffusivities are enhanced. The suppression of the relative diffusivities is caused by the resistance of the fluid between the spheres to being sheared or squeezed out of the gap.

Conversely, the diffusion of the center of mass is enhanced by the fluid entrained by one sphere pulling along the other.

The lowest order terms in Eqs. (2)–(5) would suffice to accurately describe the diffusivities when the spheres are separated by more than a few radii. Comparison with other theoretical forms which describe the diffusivities at very small separations[10] suggest that Eqs. (2)–(5) accurately describe the diffusivities over the experimental range of separations ($\rho > 2.5$).

II. EXPERIMENTAL METHOD

The experiment was conducted using commercially available polystyrene sulfate spheres with a radius of 0.966 ± 0.01 μm (Duke Scientific, Cat. No. 5095A). Such spheres typically have titratable surface charges of more than 10^5 electron equivalents and are thus surrounded by a diffuse cloud of counterions whose thickness is determined by the electrolyte's Debye-Hückel screening length. This counterion cloud can increase the hydrodynamic radius of the spheres, resulting in a diffusivity significantly smaller than suggested by Eq. (1) and the nominal radius. Furthermore, overlap of counterion clouds produces a long-range electrostatic repulsion between spheres. To eliminate the confusion that such effects might cause in this experiment, the colloid was suspended in a 0.1 mM solution of HCl. In such an electrolyte, the electrostatic and van der Waals interactions between spheres should be negligible so long as they are more than 300 nm from contact and the single-sphere diffusivities should be within 1% of that predicted by Eq. (1).

Our sample cell was constructed by sealing the edges of a No. 1 cover-slip to the surface of a glass microscope slide with uv curing epoxy. Holes drilled through the slide connect the roughly $25 \times 10 \times 0.05$ mm sample volume to two reservoirs of dilute suspension. Prior to assembly, all the glass surfaces were stringently cleaned with an acid-peroxide wash, and rinsed well with deionized water. After filling, this sample cell was placed on an Olympus IMT-2 inverted video microscope using a $100\times$, numerical aperture 1.3 oil immersion objective. A $5\times$ projection eyepiece at the camera yields a total system magnification of 85 nm per CCD pixel. At such magnification, the colloidal spheres create bright images which are broadened by diffraction to about 15 pixels in diameter. These video images were recorded on an NEC PC-VCR model S-VHS video deck during the course of the experiment.

To measure the hydrodynamic coupling between spheres, we want to study the Brownian motion of a pair of spheres which are simultaneously near each other and far from all the other spheres and the walls of the sample cell. Unfortunately, in thermally distributed dilute suspensions such isolated pairs are both rare and short-lived, making the collection of statistically large data-sets difficult and time consuming. Further complicating matters is the fact that an optical microscope only provides a two-dimensional projection of the three-dimensional distribution of spheres. While video microscopy techniques are available for estimating the spheres' position in third dimension[15] they fail if the sphere images overlap or if either sphere is more than about 1 μm out of the focal plane.

We avoided both of these difficulties by manipulating the spheres with a pair of optical gradient force traps, called optical tweezers. We can form such a trap by focusing a 30 mW, 780 nm wavelength laser beam to a diffraction-limited spot with our high numerical aperture objective lens. Near that spot the optical gradient forces acting on a sphere's light-induced electric dipole can be greater than both the thermal and radiation pressure forces, trapping it firmly in three dimensions.[8] We used two such optical traps to position a pair of colloid spheres near each other and in the same focal plane 12 μm from the lower glass wall and 40 μm from the upper wall.

We blinked the laser on and off at 6 Hz with an electromechanical shutter synchronized with the 30 Hz frame rate of our video camera. Thus we arranged for the tweezers to be turned off for three out of every five consecutive video frames. During the 110 ms interval when the tweezers are off, the spheres diffuse freely. When the tweezers are turned on, the spheres return to their trapped positions. By examining only those frames where the traps are turned off we can rapidly acquire large amounts of free diffusion data while the blinking traps hold the spheres near the desired configuration.

Furthermore, we can neglect the effect of the spheres' out of plane diffusion provided that it is small compared with their center-to-center separation. While the traps are turned off, the spheres diffuse out of the plane with an average displacement of about 350 nm. To reduce the effects of such out of plane motion, we discarded any data not acquired during the first 33 ms of a ''blink'' if the spheres were separated by less than 3 μm. This reduces the average out of plane motion for the remaining data to less than 200 nm.

During the course of the experiment, the separation between the traps was slowly increased, so that data were acquired at a range of separations. We were able to move the traps without changing their focus or introducing vignetting by varying the angle at which the beams enters the objective's back aperture.[9] A convenient method for such steering is to use a Keplerian telescope to create a plane conjugate to the objective lens' back aperture outside of the microscope body. Rotating the laser beam with a gimbal mounted mirror in that plane will move the trap about the field of view without vignetting or changing its focus.

After 100 min of video data were collected, the videotape was digitized with a Data Translation DT-3851A video digitizer installed in a 486-class personal computer. Video frames with the traps turned on were readily distinguishable by a increase in the background brightness due to scattered laser light. By controlling the video deck with the same computer, all the video frames could be digitized and the roughly 10^5 frames with the traps off could be written to disk automatically. Since the tweezers held the spheres in roughly the same position in the field of view, only a small portion of each video frame (170×80 pixels), needed to be stored and processed.

Once the images were digitized, we determined the

sphere locations by calculating the centroid of each sphere's brightness distribution in the image. This process can determine the two-dimensional coordinates of the spheres to better than 10 nm, and is described in detail elsewhere.[16] Since NTSC video is interlaced, the even and odd rows of each frame are exposed at different times, 1/60th of a second apart. Thus by determining the positions of the spheres in each set of rows (video fields) separately, we can measure their positions with a time resolution of 60 Hz.

III. RESULTS AND DISCUSSION

Some care must be taken when calculating the spheres' self-diffusivity D_0, due to the effects of the walls. For a sphere far from two parallel walls, the modified self-diffusivity is given by[17]

$$D_0' = D_0\left[1 - \frac{9a}{16x_1} - \frac{9a}{16x_2}\right], \tag{6}$$

where x_1, x_2 are the distances from the sphere to the two walls. For our sample, which was temperature regulated at 23.0 ± 0.2 °C, Eq. (1) gives $D_0 = 0.484\ \mu\text{m}^2/\text{s}$. Applying Eq. (6) yields a wall-corrected value which is 3% smaller: $D_0' = 0.470\ \mu\text{m}^2/\text{s}$.

Since the long-range flow field around a pair of comoving spheres has the same form as that for a single sphere, the same wall correction should apply. For this reason, we will use the wall-corrected self-diffusivity D_0' when calculating the center of mass diffusivities $D^{\parallel}_{\text{CM}}, D^{\perp}_{\text{CM}}$. Conversely, the flow fields far from a pair of oppositely moving spheres should partially cancel, resulting in much smaller coupling to distant walls. Thus we will use the uncorrected self-diffusivity D_0 when calculating the relative diffusivities $D^{\parallel}_{\text{RM}}, D^{\perp}_{\text{RM}}$.

To measure the diffusivities, we considered the motion of the spheres during the interval between pairs of adjacent video fields. Each blink of the optical traps lasted for six consecutive fields, providing five such pairs and thus five independent samples of the Brownian dynamics. In general, displacements caused by Brownian motion will be Gaussian distributed, with a half-width determined by the diffusivity. Specifically, the probability distribution for finding a one-dimensional displacement Δ is

$$P(\Delta) = \frac{1}{2\pi\sigma^2}\, e^{-\frac{\Delta^2}{2\sigma^2}}, \quad \text{where } \sigma = \sqrt{2D\tau} \tag{7}$$

where D is the diffusivity, τ is the time interval between position measurements and σ is the distribution's root-mean-squared (rms) deviation.

To test the Batchelor[11] formulae, Eqs. (2)–(5), we decomposed the two sphere displacements during the $\tau = 16.7$ ms interval between fields into four separate components. The motion of the spheres' center of mass between the fields was decomposed into components parallel and perpendicular to center-center line in the initial field. Similarly, the spheres' motion relative to their center of mass provided the other two components. Computing these projections on all the video field pairs in the data-set yielded 1.2×10^5 sets of four displacements.

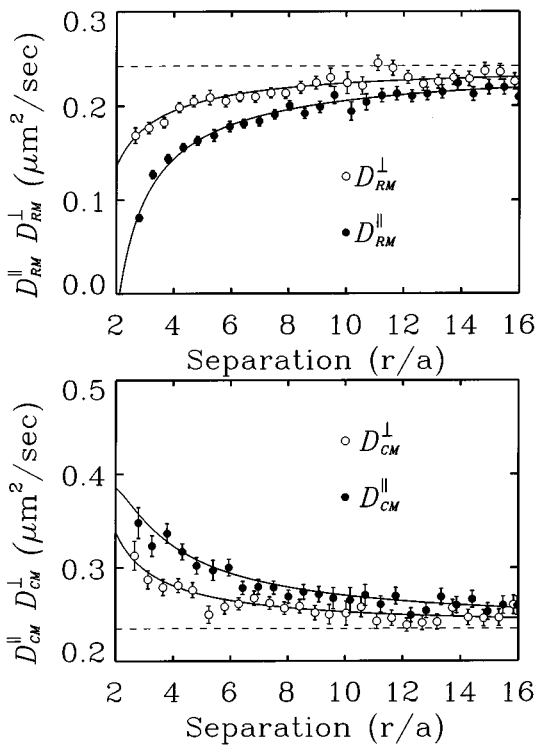

FIG. 1. The measured relative (top) and center of mass (bottom) diffusion coefficients for a pair of colloidal spheres of diameter $2a = 0.966\ \mu$m as a function of dimensionless separation ρ. The solid curves indicate the theoretical prediction given by Eqs. (2)–(5). The dashed line indicates the asymptotic diffusivity $D_0/2$ (top) and $D_0'/2$ (bottom).

The four sets of displacements were partitioned according to the initial separation of spheres in the corresponding video fields. The diffusivities were then calculated via Eq. (7) from the rms value of the displacements within each partition. The results are shown in Fig. 1, and show excellent agreement with the theory curves given by Eqs. (2)–(5).

While such joint diffusivities of the pair of spheres are clearly affected by their proximity, the effect on the self-diffusion coefficients is much more subtle, as shown in Fig. 2. Here, rather than decomposing the motion of the two spheres into a differential and a common motion, as in Fig. 1, we consider the motion of each sphere separately. The displacements were, as before, divided into a component along the center-center line, and another one perpendicular to it. These components were partitioned as before, and the corresponding diffusivities calculated from their rms values via Eq. (7).

We can determine the theoretical prediction for such self-diffusion along the center-center line by summing Eq. (2) and Eq. (4). We find that the lower order corrections cancel, leaving

$$D^{\parallel} = D_0\left[1 - \frac{15}{4\rho^4} + O(\rho^{-6})\right] \tag{8}$$

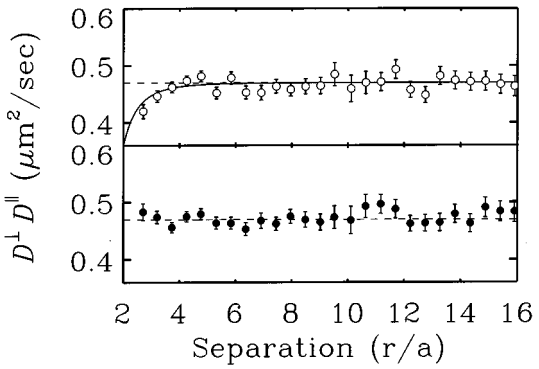

FIG. 2. The measured self-diffusion coefficients for each of a pair of colloidal diameter $2a=0.966$ μm as a function of their dimensionless separation ρ. The top plot shows the diffusion coefficients for motion perpendicular to the center-center line; the bottom one for parallel motion. The solid curve indicates the theoretical prediction given by Eq. (8). The dashed line indicates the wall-corrected, asymptotic self-diffusivity D_0'.

which is consistent with the subtle downturn seen in Fig. 2. Repeating this calculation for the perpendicular self-diffusion by summing Eq. (3) and Eq. (5), yields

$$D^{\perp}=D_0[1+O(\rho^{-6})] \tag{9}$$

showing cancellation of all the corrections up to the sixth order considered by Batchelor. This nicely accounts for our failure to observe any separation dependence of the self-diffusion coefficient $D^{\perp}$.

The cancellation of the separation dependence of the self-diffusion coefficients can be easily understood. If we consider moving only one of a pair of spheres through a viscous fluid, the other sphere is free to move in response much the same way as the parcel of fluid it displaces. At low Reynolds number inertial effects due to any difference of mass are neglected, so the only difference between the second sphere and the fluid parcel is their resistance to deformation, which is presumably responsible for the leading ρ^{-4} term in Eq. (8). The more complete cancellation for the perpendicular motion is due to the fact that in that case the motion of the second sphere, or fluid parcel, is mostly rotational rather than elongational.

By carefully examining the Brownian diffusivity of two isolated colloidal spheres, the hydrodynamic forces coupling them to one another were measured, and are in excellent agreement with theoretical expectations. These forces do not manifest themselves by a significant reduction in the magnitude of the self-diffusivity of either sphere alone. These forces do lead, however, to strong long-range correlations of the two spheres' Brownian motion.

ACKNOWLEDGMENTS

The author is pleased to acknowledge enlightening conversations with Amy Larsen and David Grier. This work was supported by the Grainger Foundation and the National Science Foundation under Grant Number DMR-9320378.

[1] Z. Adamczyk and T. G. M. van de Ven, J. Colloid Interface Sci. **96**, 204 (1983).
[2] G. F. Eveson, E. W. Hall, and S. G. Ward, Brit. J. Appl. Phys. **10**, 43 (1959).
[3] J. Happel and R. Pfeffer, A. I. Ch. E. J. **6**, 129 (1960).
[4] D. C. Prieve, S. G. Bike, and N. A. Frej, Faraday Discuss. **90**, 209 (1990).
[5] L. P. Faucheux and A. J. Libchaber, Phys. Rev. E **49**, 5158 (1994).
[6] Y. Grasselli and G. Bossis, J. Colloid Interface Sci. **170**, 269 (1995).
[7] K. Takamura, H. L. Goldsmith, and S. G. Mason, J. Colloid Interface Sci. **82**, 175 (1981).
[8] A. Ashkin, J. M. Dziedzic, J. E. Bjorkholm, and S. Chu, Opt. Lett. **11**, 288 (1986).
[9] R. S. Afzal and E. B. Treacy, Rev. Sci. Instrum. **63**, 2157 (1992).
[10] Theo G. M. van de Ven, *Colloidal Hydrodynamics* (San Diego, Academic, 1989).
[11] G. K. Batchelor, J. Fluid Mech. **74**, 1 (1976).
[12] M. Stimson and G. B. Jeffery, Proc. Roy. Soc. **111**, 110 (1926).
[13] H. Faxen, Z. Agnew. Math. Mech. **7**, 79 (1927).
[14] J. Happel and H. Brenner, *Low Reynolds Number Hydrodynamics* (Kluwer Academic, Norwell, 1991).
[15] J. C. Crocker and D. G. Grier, Phys. Rev. Lett. **73**, 352 (1994).
[16] J. C. Crocker and D. G. Grier, J. Colloid Interface Sci. **179**, 298 (1996).
[17] W. B. Russel, D. A. Saville, and W. R. Schowalter, *Colloidal Dispersions* (Cambridge University Press, Cambridge, 1989).